

THE EFFECT OF Ag_3PO_4 /GRAPHENE CO-DOPED WO_3 ELECTROCHROMIC FILM

P. KONGSONG^{a,*}, P. TATSANABENJAKUL^b, L. SIKONG^{b,c}

^a*Department of Materials Engineering, Faculty of Engineering and Architecture, Rajamangala University of Technology Isan, Nakhon Ratchasima 30000, Thailand*

^b*Department of Mining and Materials Engineering, Faculty of Engineering,*

Prince of Songkla University, Hat Yai, Songkhla, 90112, Thailand

^c*Center of Excellence in Materials Engineering (CEME),*

Prince of Songkla University, Hat Yai, Songkhla, 90112, Thailand

Ag_3PO_4 /graphene co-doped WO_3 electrochromic films were prepared by dip-coating on FTO glass substrate and annealed at 300°C for 2 h. The electrochromic properties of the films were tested by means of cyclic voltammetry. The film has an amorphous structure that positive ions and electrons can be easily inserted into the structure. As a result, the film could change the color rapidly. The Ag_3PO_4 doped WO_3 film had good optical property, i.e. for colour bleached condition, its transmittance is about 62.0%. The Ag_3PO_4 doped WO_3 sol was co-doped with graphene 0.01, 0.05 and 0.1 wt% displayed low electrochromic properties than the film undoped graphene because the reduced graphene oxide (rGO) used in this experiment had oxygen more than 8%, had low electrical property and multilayered structure.

(Received March 20, 2018; Accepted June 12, 2018)

Keywords: Electrochromic film, Tungsten trioxide film, Ag_3PO_4 /Graphene co-doped, Sol-gel method

1. Introduction

Electrochromism, a reversible and optical change, is associated with an electrochemically induced oxidation–reduction reaction after applying an appropriate potential on the electrochemical active materials. Electrochromism has received increasing interests because of its promising applications in intelligent optical displays and energy-saving smart window. Tungsten oxide has been extensively studied and can switch between transparent and blue with relatively fast response time and high coloration efficiency as compared with other electrochromic materials. The electrochromic process, well known in tungsten oxide, is promoted by the injection and extraction of electrons and H^+ or Li^+ cations, resulting in color change. The switching time and intensity of color change in tungsten oxide strongly rely on the availability of electrons to facilitate the $\text{W}^{6+} \leftrightarrow \text{W}^{5+}$ redox reaction. When electrons and cations are injected, the electronic structure of WO_3 is modified, and the Fermi level is moved upward. As a result, excess electrons fill the t_{2g} band of WO_3 , and the color of tungsten changes from transparent to blue [1].

The fabrication of tungsten trioxide thin films for electrochromic applications have been widely studied by evaporation, sputtering, anodization and sol-gel methods [2]. Many studies have been done on the synthesis of tungsten trioxide films by sol-gel method [3-4] due to its low cost, and unique deposition technique which gives homogenous coating on relatively large glass substrate. A popular precursor for the tungsten oxide sol is solid peroxotungstic acid prepared from tungstic acid via sodium tungstate dihydrate or directly from tungsten or tungsten carbide powder dissolution in hydrogen peroxide solution [5].

*Corresponding author: physics_psu@windowslive.com

Generally, the electrochromic properties of tungsten trioxide can be improved by doping some elements or chemical compounds such as graphene, MWCNTs, VO_2 , TiO_2 , Ag_3PO_4 , Ag, etc. In this study, Ag_3PO_4 and graphene were added to improve properties of the electrochromic films, since it has been reported to be good photocatalyst having photo-oxidation properties [1, 6-10].

Graphene, with one-atom thick sheet and two-dimensional structure, is a very promising candidate for improving the physical and chemical properties of composites. The promising characteristics of graphene such as high electrical conductivity and large surface area, endow its composites with multifaceted functionalities. We envisaged that the synergistic incorporation of graphene into WO_3 will enable the enhanced electrochromic performance by overcoming the intrinsic drawback of WO_3 as electrochromic materials. [1]. Reduced graphene oxide (rGO) is the advanced materials that structure with the monolayer of carbon atom packed into a 2D honeycomb lattice exhibiting high photocatalytic performance because of its high electrical conductivity, excellent mobility of charge carriers ($20,000 \text{ cm}^2/\text{Vs}$. at room temperature) and large specific surface area ($2,630 \text{ m}^2/\text{g}$). The semiconductor doped with rGO shows high photocatalytic performance due to its excellent electron acceptor that can retard the recombination of the electron-hole pair and now are applied for the photocatalyst, gas sensors, and energy conversion [11].

In this paper, the effect of graphene content on WO_3 electrochromic film prepared by sol-gel method was investigated and characterized by scanning electron microscopy (SEM), UV-vis spectrophotometer, and X-ray photo-electron spectroscopy (XPS). The electrochromic properties of synthesized films were carried out by cyclic voltammetry (CV) and UV-Vis spectrophotometry methods.

2. Experimental

2.1 Synthesis

2.1.1 WO_3 sol synthesis

The WO_3 sol was synthesized from tungsten powder by sol-gel method. Tungsten powder (6.5 g; 99.9%, Merck) was dissolved into a mixture of 4 mL distilled water and 40 mL of 30% hydrogen peroxide to form a colorless peroxotungstic acid (PTA) precursor [12]. The coating sol was prepared by mixing 10 mL of the PTA solution with 10 mL of ethanol with 1 h stirring. Subsequently, the WO_3 sol was obtained and kept for making coating sol.

2.1.2 Ag_3PO_4 powder synthesis

The Ag_3PO_4 powder was synthesized by precipitate method. $\text{Na}_2\text{HPO}_4 \cdot 12\text{H}_2\text{O}$ (Ajex Finechem Pty. Ltd) and $\text{NaH}_2\text{PO}_4 \cdot 2\text{H}_2\text{O}$ (Ajex Finechem Pty. Ltd) were mixed to obtain a phosphate buffer solution. The buffer solution was then added to a 20 mL of 10 mM solution of AgNO_3 and stirred for 10 minutes, in which yellow Ag_3PO_4 precipitates were formed. The precipitates were then washed for several times and dried at 60°C to obtain Ag_3PO_4 powders for doping in WO_3 sol. [13].

2.1.2 Reduction of GO

Graphene oxide (GO) was prepared using natural graphite powder through a modified Hummers method [14]. GO was reduced by the chemical reduction method. The 0.5 g of GO and 100 mL of 0.5% NH_4OH (37%, J.T. Baker) were mixed and stirred at 60°C for 30 min until the dispersion turned yellow-brown, then 4 mM ascorbic acid (99.5%, Poch) was mixed and kept at 95°C for 60 min. The mixture was filtered and washed with distilled water and ethanol until pH ~ 6 , then the product was collected and mixed with 100 mL of distilled water to make 5 mg/mL rGO dispersion [11].

2.1.3. Ag_3PO_4 /grapheme co-doped WO_3 sol synthesis

The coating sol was prepared by adding Ag_3PO_4 powder 0.8 wt% [15] and graphene 0.00, 0.01, 0.05 and 0.1 wt% into the WO_3 sol and stirred for 1 h. The solution was aged for 24 h before

coating. The sol was deposited on cleaned Fluoride doped tin oxide (FTO) coated glasses ($7 \Omega/\text{sq.}$, Sigma-Aldrich) with a dimension of $2.5 \times 2.5 \times 0.23 \text{ cm}^3$ by dip coating at the dipping speed of 0.1 mm/s . The as-deposited films were allowed to dry at room temperature for 24 h and annealed at $300 \text{ }^\circ\text{C}$ for 2 h at the rate of $5 \text{ }^\circ\text{C/min}$. Then the sample was allowed to cool in ambient temperature.

2.2. Characterization techniques

X-ray diffraction (XRD, X'Pert MPD, Philips, Netherlands) was performed by a diffractometer with Cu $K\alpha$ radiation to examine the structure of the annealed films. The surface morphology of the annealed tungsten oxide films was observed using Scanning electron microscopy (SEM, Quanta 400). The transmittance spectra were recorded by a UV-Vis spectrophotometer (UV-2401, Shimadzu) with air as a reference. Cyclic voltammetry tests were performed in a three cell configuration with the electrochromic film, Pt and Ag/AgCl as the working, counter and reference electrodes, respectively. The electrolyte was 0.5 M sulfuric acid (H_2SO_4). The voltammetric cycle was performed at the voltages between -1.0 and 1.0 V relative to Ag/AgCl with a scan rate 100 mV/s . The current was recorded at cycle 1 under the conditions as described above. X-ray photo-electron spectroscopy (XPS; AXIS ULTRA^{DLD}, Kratos analytical, Manchester UK.) was used to determine the Ag^+ and W^{6+} ions state of the electrochromic films.

3. Results and discussion

3.1 Structural properties

Fig. 1 shows the XRD diffraction patterns of Ag_3PO_4 -doped WO_3 film and Ag_3PO_4 /graphene co-doped WO_3 films coated on FTO substrate. It was noticed that all films were amorphous. The peaks were identified at the 2θ is 26.59° , 33.89° , 37.91° , 51.71° , 54.65° and 61.63° . The diffraction peaks can be indexed to the SnO_2 phase of the FTO substrate. [16]

The SEM of $\text{WO}_3/0.8 \text{ wt\% Ag}_3\text{PO}_4$, $\text{WO}_3/0.8 \text{ wt\% Ag}_3\text{PO}_4/0.01 \text{ wt\% rGO}$, $\text{WO}_3/0.8 \text{ wt\% Ag}_3\text{PO}_4/0.05 \text{ wt\% rGO}$, $\text{WO}_3/0.8 \text{ wt\% Ag}_3\text{PO}_4/0.10 \text{ wt\% rGO}$ films, a cross-section of the $\text{WO}_3/0.8 \text{ wt\% Ag}_3\text{PO}_4$ films and rGO are shown in Fig. 2. Fig 2 (a) shows the uniform surface with Ag_3PO_4 small particles on the $\text{WO}_3/\text{Ag}_3\text{PO}_4$ film. Fig 1 (b, c and d) show graphene sheets on the $\text{WO}_3/0.8 \text{ wt\% Ag}_3\text{PO}_4$ film. Fig 2 (e) shows a cross-section of the $\text{WO}_3/\text{Ag}_3\text{PO}_4$ films of 625 nm thickness. We also used the chemical reduction method to rGO for control experiment, and the SEM image of rGO structure in Fig. 2 (f) demonstrates that this reduction process with NH_4OH and ascorbic acid as the reductive agent is effective to produce graphene sheets with thin layers.

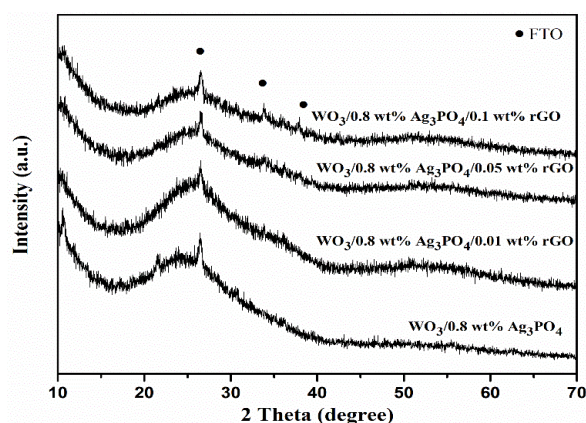


Fig. 1. The x-ray diffraction patterns of (a) $\text{WO}_3/0.8 \text{ wt\% Ag}_3\text{PO}_4$, (b) $\text{WO}_3/0.8 \text{ wt\% Ag}_3\text{PO}_4/0.01 \text{ wt\% rGO}$, (c) $\text{WO}_3/0.8 \text{ wt\% Ag}_3\text{PO}_4/0.05 \text{ wt\% rGO}$ and (d) $\text{WO}_3/0.8 \text{ wt\% Ag}_3\text{PO}_4/0.10 \text{ wt\% rGO}$ films.

Fig. 3 (a and b) show the X-ray photoelectron spectroscopic (XPS) survey spectra of $\text{WO}_3/0.8 \text{ wt}\% \text{Ag}_3\text{PO}_4$ and $\text{WO}_3/0.8 \text{ wt}\% \text{Ag}_3\text{PO}_4/0.01 \text{ wt}\% \text{rGO}$ films. The elements W, O, Ag and C were clearly detected. Fig. 3 (c) shows the existence of Ag in two bands corresponding to 368.2 and 374.2 eV, this ascribes to $\text{Ag } 3d_{5/2}$, and $\text{Ag } 3d_{3/2}$, respectively. Fig. 3 (d) shows the existence of Ag in two bands corresponding to 368.4 and 374.5 eV, this ascribes to $\text{Ag } 3d_{5/2}$ and $\text{Ag } 3d_{3/2}$, respectively. These bands correspond to the Ag^+ of Ag_3PO_4 [13, 16]. Fig. 3(e and f) show spectra of the W-4f core level of WO_3 , $\text{WO}_3/0.8 \text{ wt}\% \text{Ag}_3\text{PO}_4$ and $\text{WO}_3/0.8 \text{ wt}\% \text{Ag}_3\text{PO}_4/0.01 \text{ wt}\% \text{rGO}$. A slight shift of the W-4f binding energies toward higher energies was observed in the $\text{WO}_3/0.8 \text{ wt}\% \text{Ag}_3\text{PO}_4$ and $\text{WO}_3/0.8 \text{ wt}\% \text{Ag}_3\text{PO}_4/0.01 \text{ wt}\% \text{rGO}$. The spectra of the $\text{WO}_3/0.8 \text{ wt}\% \text{Ag}_3\text{PO}_4$ had spin orbit doublet peaks at 36.1 eV ($\text{W-}4f_{7/2}$) and 38.2 eV ($\text{W-}4f_{5/2}$). The spectra of the $\text{WO}_3/0.8 \text{ wt}\% \text{Ag}_3\text{PO}_4/0.01 \text{ wt}\% \text{rGO}$ had spin orbit doublet peaks at 36.2 eV ($\text{W-}4f_{7/2}$) and 38.4 eV ($\text{W-}4f_{5/2}$) [10]. From band gap measurements, Ag_3PO_4 doping reduced the band gap energy from 2.79 eV of pure WO_3 to 2.69 eV of $\text{WO}_3/0.8 \text{ wt}\% \text{Ag}_3\text{PO}_4$ samples [15]. Fig. 3 (a and b) show the high-resolution XPS spectra of (a) C 1s on the $\text{WO}_3/ \text{WO}_3/0.8 \text{ wt}\% \text{Ag}_3\text{PO}_4/0.01 \text{ wt}\% \text{rGO}$ and (b) C 1s on the rGO sheets. From the figure, we can see that it also exhibits the same oxygen functionalities. Although the C1s XPS spectrum of rGO also exhibits these oxygen functional groups, their peak intensities were much weaker than those in GO. The films displayed low electrochromic properties than the film undoped graphene because the rGO used in this experiment had oxygen more than 8%, has low electrical property and multilayered structure [17]

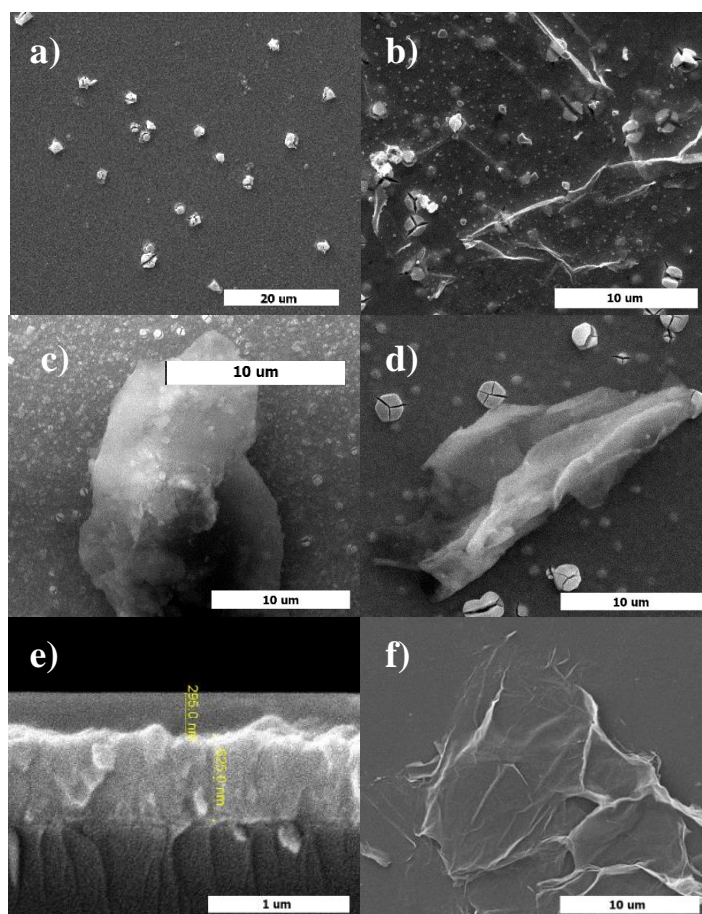


Fig. 2. The SEM images of (a) $\text{WO}_3/0.8 \text{ wt}\% \text{Ag}_3\text{PO}_4$, (b) $\text{WO}_3/0.8 \text{ wt}\% \text{Ag}_3\text{PO}_4/0.01 \text{ wt}\% \text{rGO}$, (c) $\text{WO}_3/0.8 \text{ wt}\% \text{Ag}_3\text{PO}_4/0.05 \text{ wt}\% \text{rGO}$, (d) $\text{WO}_3/0.8 \text{ wt}\% \text{Ag}_3\text{PO}_4/0.10 \text{ wt}\% \text{rGO}$ (e) a cross-section of the $\text{WO}_3/0.8 \text{ wt}\% \text{Ag}_3\text{PO}_4$ films and rGO sheet.

3.2 Electrochromic performance evaluation

Fig.4 shows the cyclic voltammograms of Ag_3PO_4 -doped WO_3 film and Ag_3PO_4 /grapheme co-doped WO_3 films in 0.5 M H_2SO_4 solution at a scan rate of 100 mVs^{-1} . The $\text{WO}_3/0.8 \text{ wt}\%$ Ag_3PO_4 film displayed significantly higher current density than Ag_3PO_4 /grapheme co-doped WO_3 films. Since the films had same thickness, increase in current density is due to Ag_3PO_4 doping [10]. This indicates that more ions and electrons were transferred at the interface between the $\text{WO}_3/0.8 \text{ wt}\%$ Ag_3PO_4 film and electrolyte. The diffusion coefficient (D) was calculated using Randles-Sevcik equation [4]. It was found that 0.8 wt% Ag_3PO_4 -doped WO_3 film exhibited higher diffusion coefficient ($8.56 \times 10^{-11} \text{ cm}^2/\text{s}$) than the Ag_3PO_4 /grapheme co-doped WO_3 films, leading to its greater electrochromic effect (Table 1). The films displayed low electrochromic properties than the film undoped graphene because the rGO used in this experiment had oxygen more than 8%, with low electrical property and multilayered structure.

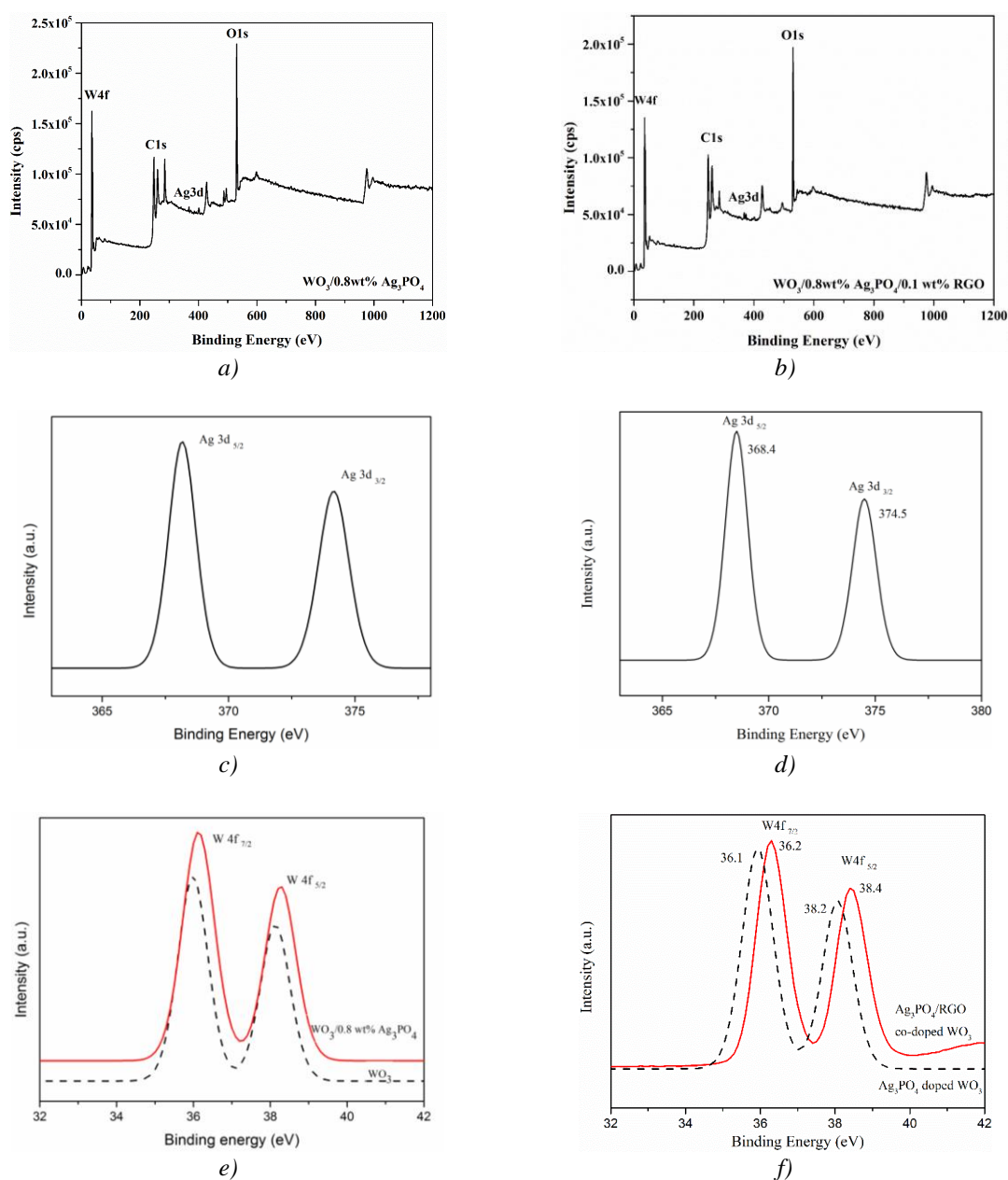


Fig. 3 The XPS spectra of (a) $\text{WO}_3/0.8 \text{ wt}\%$ Ag_3PO_4 ; (b) $\text{WO}_3/0.8 \text{ wt}\%$ $\text{Ag}_3\text{PO}_4/0.01 \text{ wt}\%$ rGO; (c) Ag 3d on the $\text{WO}_3/0.8 \text{ wt}\%$ Ag_3PO_4 ; (d) Ag 3d on the $\text{WO}_3/0.8 \text{ wt}\%$ $\text{Ag}_3\text{PO}_4/0.01 \text{ wt}\%$ rGO; (e) W 4f on the $\text{WO}_3/0.8 \text{ wt}\%$ Ag_3PO_4 ; (f) W 4f on the $\text{WO}_3/0.8 \text{ wt}\%$ $\text{Ag}_3\text{PO}_4/0.01 \text{ wt}\%$ rGO films.

Table 1. Diffusion coefficient of Ag_3PO_4 -doped WO_3 film and Ag_3PO_4 /grapheme co-doped WO_3 films.

Sample	Diffusion coefficient, D (cm^2/s)
$\text{WO}_3/0.8 \text{ wt}\% \text{ Ag}_3\text{PO}_4$	8.56×10^{-11}
$\text{WO}_3/0.8 \text{ wt}\% \text{ Ag}_3\text{PO}_4/0.01 \text{ wt}\% \text{ rGO}$	4.79×10^{-11}
$\text{WO}_3/0.8 \text{ wt}\% \text{ Ag}_3\text{PO}_4/0.05 \text{ wt}\% \text{ rGO}$	2.04×10^{-11}
$\text{WO}_3/0.8 \text{ wt}\% \text{ Ag}_3\text{PO}_4/0.1 \text{ wt}\% \text{ rGO}$	1.25×10^{-11}

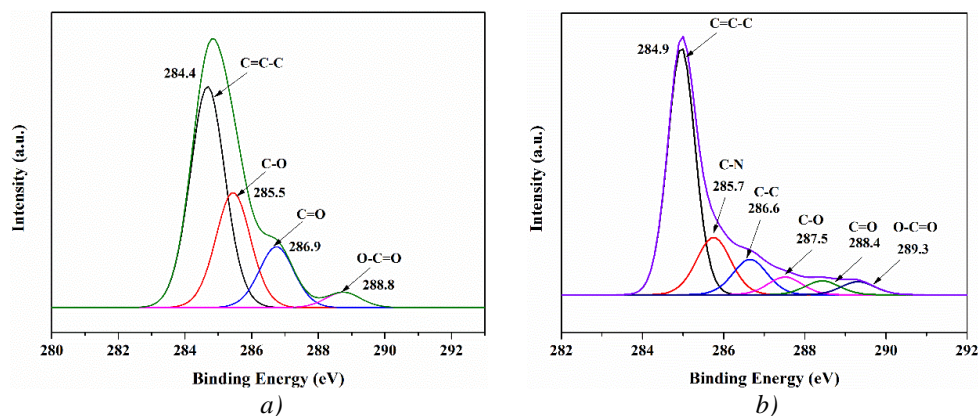


Fig. 3. The high-resolution XPS spectra of (a) C 1s on the $\text{WO}_3/0.8 \text{ wt}\% \text{ Ag}_3\text{PO}_4/0.01 \text{ wt}\% \text{ rGO}$ film; (b) rGO sheet.

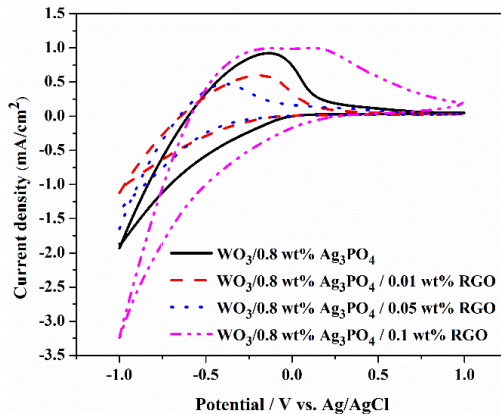


Fig. 4. Cyclic voltammograms of $\text{WO}_3/0.8 \text{ wt}\% \text{ Ag}_3\text{PO}_4$, $\text{WO}_3/0.8 \text{ wt}\% \text{ Ag}_3\text{PO}_4/0.01 \text{ wt}\% \text{ rGO}$, $\text{WO}_3/0.8 \text{ wt}\% \text{ Ag}_3\text{PO}_4/0.05 \text{ wt}\% \text{ rGO}$ and $\text{WO}_3/0.8 \text{ wt}\% \text{ Ag}_3\text{PO}_4/0.10 \text{ wt}\% \text{ rGO}$ films in $0.5 \text{ M H}_2\text{SO}_4$ solution at a scan rate of 100 mVs^{-1} .

UV-vis transmittance spectra between 300-900 nm of the $\text{WO}_3/0.8 \text{ wt}\% \text{ Ag}_3\text{PO}_4$, $\text{WO}_3/0.8 \text{ wt}\% \text{ Ag}_3\text{PO}_4/0.01 \text{ wt}\% \text{ rGO}$, $\text{WO}_3/0.8 \text{ wt}\% \text{ Ag}_3\text{PO}_4/0.05 \text{ wt}\% \text{ rGO}$ and $\text{WO}_3/0.8 \text{ wt}\% \text{ Ag}_3\text{PO}_4/0.10 \text{ wt}\% \text{ rGO}$ films were measured at 1.0 V (bleached state) and -1.0 V (colored state) in H_2SO_4 0.5 M solution. It can be seen that all the films displayed low transmittance at -1.0 V and high transmittance at 1.0 V. The transmission spectra of the four films are shown in Fig. 5 and Table 2. The optical modulations (difference of % transmittance, ΔT) of the films were compared at wavelength 631 nm. The ΔT of $\text{WO}_3/0.8 \text{ wt}\% \text{ Ag}_3\text{PO}_4$ was the highest and higher than that of Ag_3PO_4 /grapheme co-doped WO_3 films due to the more ions and electrons transferred at the interface between the $\text{WO}_3/0.8 \text{ wt}\% \text{ Ag}_3\text{PO}_4$ film and electrolyte as mentioned above.

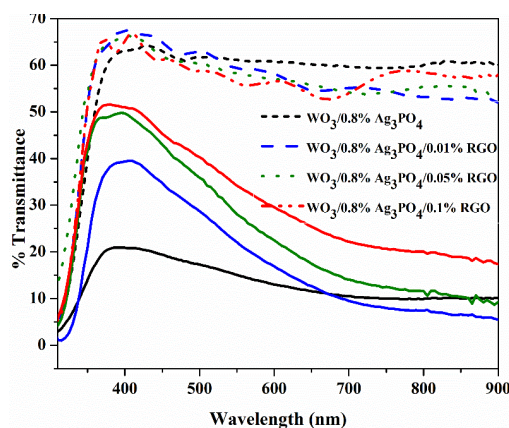


Fig. 5. UV-Vis transmittance spectra of $WO_3/0.8 \text{ wt}\% Ag_3PO_4$, $WO_3/0.8 \text{ wt}\% Ag_3PO_4/0.01 \text{ wt}\% rGO$, $WO_3/0.8 \text{ wt}\% Ag_3PO_4/0.05 \text{ wt}\% rGO$ and $WO_3/0.8 \text{ wt}\% Ag_3PO_4/0.10 \text{ wt}\% rGO$ films measured at 1.0 V (bleached state) and -1.0 V (colored state) in 0.5 M H_2SO_4 solution.

Table 2. The transmission spectra of 0.8 wt% Ag_3PO_4 -doped WO_3 film and Ag_3PO_4 /grapheme co-doped WO_3 films.

% Transmittance	T_b (%)	T_c (%)	ΔT
$WO_3/0.8 \text{ wt}\% Ag_3PO_4$	62.0	14.8	47.2
$WO_3/0.8 \text{ wt}\% Ag_3PO_4/0.01 \text{ wt}\% rGO$	60.1	23.3	36.8
$WO_3/0.8 \text{ wt}\% Ag_3PO_4/0.05 \text{ wt}\% rGO$	58.9	29.8	29.1
$WO_3/0.8 \text{ wt}\% Ag_3PO_4/0.1 \text{ wt}\% rGO$	57.7	35.3	22.4

4. Conclusions

The Ag_3PO_4 /grapheme co-doped WO_3 electrochromic films were successfully prepared from tungsten trioxide precursor and silver orthophosphate powder, and were deposited on FTO glass substrate by sol-gel and dip coating method. $WO_3/0.8 \text{ wt}\% Ag_3PO_4$ films showed the highest optical transmittance difference and it had good reversibility, and fast switching time as compared to Ag_3PO_4 /grapheme co-doped WO_3 films. The Ag_3PO_4 doped WO_3 sol was co-doped with graphene displaying low electrochromic properties than the film undoped graphene because the rGO used in this experiment had low electrical property and multilayered structure. Since the electrochromic properties are enhanced by Ag_3PO_4 doping, this work can be used to improve the performance of smart windows and screens.

Acknowledgments

The author would like to thank the Faculty of Engineering, Prince of Songkla University for the financial support under the contacts number ENG-57-2-7-02-0197-S, the Center of Excellence in Materials Engineering (CEME), Prince of Songkla University, and the Department of Materials Engineering, Faculty of Engineering and Architecture, Rajamangala University of Technology Isan. Dr. Mcwinner Yawman is also acknowledged for his comments and suggestions, as he is the Research & Publication Expert and Trainer of the Institute of Research and Development Rajamangla University of Technology Isan.

References

- [1] C. Fu, C. Foo, P.S. Lee, *Electrochim. Acta* **117**, 139 (2014).
- [2] E. Cazzanelli, M. Castriota, R. Kalendarev, A. Kuzmin, J. Purans, *Ionics* **9**, 95 (2003).
- [3] H. M. A. Soliman, A. B. Kashyout, Mohamed S. El Nouby, A. M. Aboshely, *Int. J. Electrochem. Sci.* **7**, 258 (2012).
- [4] K. Dong Lee, *Sol. Energy Mater. Sol. Cells* **57**, 21 (1999).
- [5] A. Patra, K. Auddy, D. Ganguli, J. Livage, P.K. Biswas, *Mater. Lett.* **58**, 1059 (2004).
- [6] G. Leftheriotis, S. Papaefthimiou, P. Yianoulis, A. Siokou, D. Kefalas, *Appl. Surf. Sci.* **218**, 275 (2003).
- [7] C. K. Lin, S. C. Tseng, C. H. Cheng, C. Y. Chen, C. C. Chen, *Thin Solid Films* **520**, 1375 (2011).
- [8] L. Cai, X. Xiong, N. Liang, Q. Long, *Appl. Surf. Sci.* **353**, 939 (2015).
- [9] N. K. Eswar, P. C. Ramamurthy, G. Madras, *Photochem. Photobiol. Sci.* **14**, 1223 (2015).
- [10] S. Adhikari, Y. Y. Song, Y. M. Wang, M. Niraula, K. Cho, S. K. Dhungel, Z. D. Gao, N. K., Shrestha, S. H. Han, *Opt. Mater.* **40**, 112 (2015).
- [11] L. Sikong, P. Choopool, K. Kooptarnond, *Dig. J. Nanomater. Biostruct.* **11**(3), 821 (2016).
- [12] C. L. Wu, C. K Wang, C. K. Lin, S. C. Wang, J. L. Huang, *Surf. Coat. Technol.* **231**, 403 (2013).
- [13] A. Wu, C. Tian, W. Chance, Y. Hong, Q. Zhang, Y. Qu, H. Fu, *Mater. Res. Bull.* **48**, 3043 (2013).
- [14] S. Stankovich, D. A. Dikin, G. H. B. Dommett, K. M. Kohlhaas, E. J. Zimney, E. A. Stach, R. D. Piner, S. T. Nguyen, R. S. Ruoff, *Nature* **442**, 282 (2006).
- [15] P. Tatsanabekkul, L. Sikong, K. Chetpattananondh, *Key Engineering Materials* **707**, 139 (2016).
- [16] B. Zhao, S. Lu, X. Wang, J. Liu, H. Yan, *Ionics* **2**, 261 (2016).
- [17] S. Pei, H. M. Cheng, *Carbon* **50**, 3210 (2012).